DEVELOPMENT OF WIDE DYNAMIC RANGE BEAM LOSS MONITOR SYSTEM FOR J-PARC MAIN RING

K. Satou†, T. Toyama, N. Kamikubota, S. Yamada, J-PARC/KEK, Ibaraki, Japan
S. Yoshida, Kanto Information Service, Ibaraki, Japan

Abstract

The new beam loss monitor (BLM) system now in operation at the main ring of J-PARC consists of an isolated front-end current to voltage converter, a VME-based 24 bit ADC system. A dual detector system employs a proportional-type gas chamber (PBLM) and an air-filled ionization chamber (AIC). The system shows a wide dynamic range of 160 dB. It can detect the low level signal that would arise in the case of the detection of residual dose in the ring itself after the beam has been turned off as well as an event such as high level beam loss at the collimators. The signal rise time of the waveform obtained is 17 μs which is fast enough to meet the speed requirement of the Machine Protection System (MPS); which is that the MPS should dump the beam within 100 μs when the beam loss signal exceeds the reference levels set in the ADC system.

INTRODUCTION

The new BLM system was designed [1] to meet the conditions and the requirements listed below. Some items were modified as we tested how the system worked with various beam tunings.

1. The system is required to detect losses from the weak beams that are passed round the ring during the beam commissioning phase, when the beam intensity is only 1 % of the designed maximum intensity of 4E13 protons per bunch (eight bunches for full).
2. The system must be able to detect an unusual loss of power in the beam and send an alarm to the Machine Protection System (MPS) [2] to dump the beam within 100 μs.

   Acceptable beam power loss in the main ring (MR) is 0.5 W/m in the arc sections, 2 kW at the collimators, 7.5 kW at the slow extraction (SX) section, and 1.125 kW at the fast extraction (FX) section [3, 4].
3. Independently of loss of power in the beam, the level of activation of the components should be kept within the limits set for workers to perform hands-on maintenance. Each device should display the levels that should not be exceeded for various maintenance operations including unscheduled and urgent repair-works for a malfunction of the device. The worker's daily radiation exposure dose is limited to 0.5 mSv for men and 0.3 mSv for women in J-PARC.
4. The activations have to be measured after the beam has been turned off. We need to be able to detect residual doses as low as 10 μSv/h. On the other hand the expected dose for the detectors in the collimator section was estimated to be 0.053 Gy/Cycle for 2kW beam power lost uniformly in the collimators [5]. To achieve this, the monitoring system must have a dynamic range wider than 120 dB [1].
5. The bandwidth needed to monitor turn-by-turn beam losses for the system is from DC to 200 kHz. To study the head-tail instability [6], detection of even higher frequency signals of about 100 MHz would be needed.

The new BLM system has been in operation since last summer 2016 with a dynamic range of the system wider than 160 dB. However the system's bandwidth is limited: it goes from DC to 10 kHz. To meet requirement 5, we are currently working on a new detector system. In this paper, the performance of the present BLM system is described.

DETECTORS

We incorporated three types of detector: a cylindrical proportional gas chamber (PBLM), a 1 m long short-type air ionization chamber (sAIC), and a long-type air ionization chamber (longAIC). The maximum gas gain of the PBLM is 2E4 at a bias voltage of −2.0 kV. The 216 PBLMs and the 53 sAICs (only in the straight sections) are mounted at each quadrupole magnet (QM) as shown in Fig. 1. They stand 360 mm away from the QM surface and 848 mm from the centre of the beam duct. The number labelled on each BLM corresponds to the address number of the MR.

A magnetic shield made of iron suppresses perturbation in the gas gain of the PBLM due to leakage of magnetic field from the QM. Another 19 longAICs were installed on the cable rack running on the outside wall of the MR tunnel to cover whole MR ring. The distance between the detectors and centre of the beam duct is 3 m.

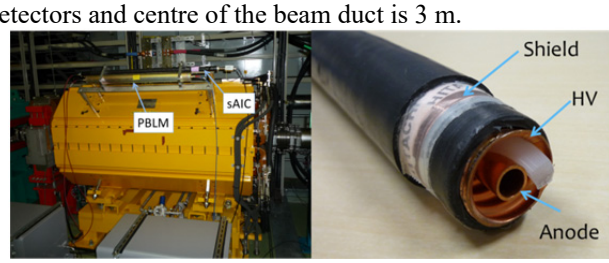

Figure 1: Left) Photo of the PBLM and sAIC. Right) Cable structure used for AIC.

HV System

To feed a bias voltage to each BLM detector, the MR area was divided into nine sections; these are Injector and Collimator section (#213-20), 1st half of Arc A (#21-44), 2nd half of Arc A (#45-68), SX section (#69-92), 1st half of Arc B (#93-116), 2nd half of Arc B (#117-140), RF & FX section (#141-164), 1st half of Arc C (#165-188), 2nd half of Arc C (#189-212), where (#a-b) means the area

† email address kenichirou.satou@j-parc.jp

from address a to b. In each section, detectors are grouped and the HV cables are daisy-chained so that the PBLMs in each section are thus operated with the same bias voltage. The bias voltages for the AICs are, however, all set at −500 V. During operations, the output currents of the power supplies are less than 0.1 mA which are much less than the maximum output current of 20 mA. The drift of the HV of the power supply is less than 0.03 %.

PBLM

The PBLMs have been used as the main detectors. They offer a wide range in gas gain and a fast impulse response about 0.1 μs. Post-signal processing takes place within the signal rise time of 17 μs, well within the MPS speed requirement. The details of the PBLM are described in refs. [5, 7, 8].

The initial charge induced by the beam loss is amplified by the gas gain. The output current divided by the gas gain can be used as an indication of beam loss signal. By changing the bias setting, a wide dynamic range can be covered. However an increase of the output current decreases the gas gain [9]. For example 1 μA and 10 μA output DC current results in 4 % and 40 % gain decrease in case of the bias voltage of −1.6 kV, respectively. This means that the PBLMs are likely to underestimate the beam power loss especially in the Injector and Collimator section and the SX section where a large beam loss is inevitable.

sAIC and longAIC

The AIC is an ion chamber that uses a double shielded 20D coaxial cable. A corrugated Cu pipe acts as an inner shield core while spiral polyethylene acts as an insulator as shown in Fig. 1. The centre Cu tube picks up the charge, while the bias voltage is applied on the corrugated pipe tube and the outermost Cu tape shield is grounded.

The sAIC is a 1 m long AIC. The maximum output current and sensitivity were checked by gamma rays from a strong ^{60}Co gamma source. The data shows linear response up to 10 μA within an uncertainty of about 10 %. The output current corresponds to 3.2 kGy/h [1], so the sensitivity is 11 μC/Gy. This qualifies the sAIC for use in high radiation environment.

The longAICs are, on average, 84 m long. The 19 longAICs cover the whole length of the MR tunnel. They measure average beam power loss to ensure that the beam loss is lower than the criteria of the item 2 listed in the introduction. The calibration was made using intentional beam losses of the injection beam at the collimator units, and in the Arc A and the Arc B. The beam losses were generated by the local bump orbit. The beam energy was fixed as 3GeV. The number of the lost particles was measured by the DCCT [8]. The longAIC#1-10 outputted 14.1 nC for the beam loss of the 1.1E11±0.2E11 protons at the collimators. The detector covers the area from the injection point of address #1 to the end of the collimator units of address #10. The efficiency, which is the output charge divided by the beam power lost, is thus 1/3.6 μC/kJ. In the Arc sections, it was 1/8.9 μC/kJ on average.

THE FRONT-END AMP AND ADC

A new data acquisition system was developed and installed during the maintenance period last summer 2016. It consists of an isolated current-to-voltage converter that uses photo-couplers (front end amp) and a VME-based 24 bit ADC system. The system is described in ref. [10].

The conversion factor and the −3 dB bandwidth of the front end amp are 1 V/μA and 50 kHz, respectively. The maximum input current is 10 μA. To improve the signal to noise ratio, a low-pass filter of 10 kHz is currently inserted in the front-end amp.

An ADC system with a noise level of 100 μVpp and a total harmonic distortion of 80 dB was developed. The effective number of bits is 16.5. To improve the ground level stability, offset subtraction is performed at each cycle. After the offset subtraction, the ADC digitized at the rate of 1 MS/s. Each digitized point is sequentially compared with a reference level. At the same time, the data is summed and compared with the second reference level. When the data indicates one of the reference levels has been exceeded, the system outputs an alarm to the MPS system within 2 μs. The 1 MS/s waveform data is then down-converted to 1 KS/s data.

BLM DATA

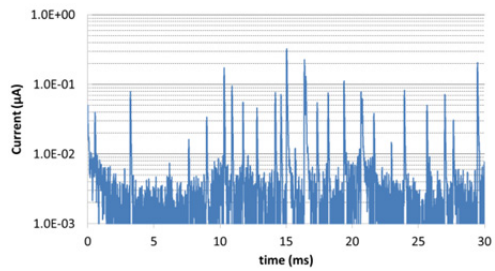

Figure 2: Pulse signal from the PBLM induced by the gamma rays from the activated magnet.

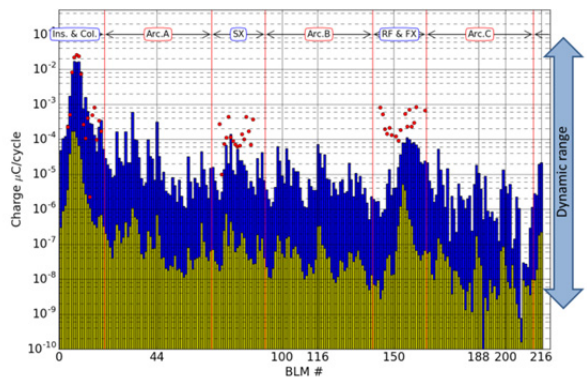

Figure 3: Integrated charge plot. The beam loss signals from PBLMs and sAICs are shown as blue bars and red solid circles, respectively. The yellow bars show the residual dose.

To check the impulse response of the system, the gamma rays from the activated magnet were measured. The

ISBN 978-3-95450-182-3

1 MS/s waveform data are shown in Fig. 2, where the bias voltage was −2.0 kV. The pulses can be seen in the figure. The 10-90 % rise time is 17 µs.

The following data were obtained on the FX mode operation with 460 kW output power. The operation-cycle was 2.48 s long.

The integrated charge data of the PBLMs and sAICs are shown in Fig. 3. The gas gains of the PBLMs were corrected for the data in this plot. The beam loss signals from PBLMs are shown as blue bars. The bias voltage of the PBLMs was all −1.6 kV except for these in the Injector and Collimator section whose bias voltage was −1.3 kV. The gas gain is 628 and 61, respectively, for bias voltages of −1.6 and −1.3 kV. The sAIC data are shown as red solid circles. The data shows that its detection threshold is about 1E−3 nC/Cycle.

The residual dose data measured five hours after the beam was shut down are shown as yellow bars, where the bias voltage was −2.0 kV. The integration time was 1.6 s. The data were compared with the measurements by using the commercial dose meter, CANBERRA RADIAGEM2000. The output charge of 1.2E−5 µC/Cycle corresponds to the residual dose rate of 100 µSy/h.

The 1 kS/s waveforms of the PBLMs were divided by each gas gain and displayed in a contour plot as shown in Fig. 4. The post signal processing, a simple averaging process for data points in the time window of 20 ms which is shifted by a 10 ms interval, was adopted to reduce noise due to the fundamental and the higher harmonics coming from the 50 Hz AC supply.

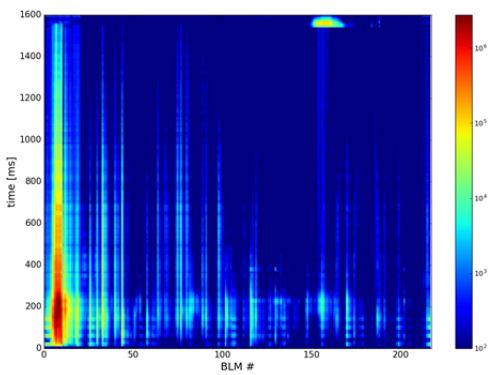

Figure 4: Contour plot of the waveforms from the PBLMs.

We can see in the figure the key details of the beam losses: positions, timings, and intensities. An intense beam loss at the collimators can be seen at the time around 200 ms which is due to the imperfection of the momentum tracking of the bending magnets occurred after the acceleration start. And the extraction beam loss at the FX septum magnet can be seen around BLM#156. Four times losses can also be seen at 0 ms, 40 ms, 80 ms, and 120 ms after the beam injection. These losses were caused by injection miss-matches.

DISCUSSION

At the outset of the design process, the target for the rise time was 10 µs for the MPS system to dump the beam within 100 µs. However, it seems to us that the present rise time of 17 µ s is fast enough. We took into-consideration the observations that the cable delay is a few µs, the processing time of the ADC system is about 2 µs, and the processing time of the MPS system is about 1 µs.

The 1 KS/s waveforms of PBLM#8 sAIC#8, and longAIC#1-10 are shown in Fig. 5. The gas gains were not corrected for these waveforms. As shown in the figure, the waveform of the PBLM is saturated at the output current of 10 µA. On the other hand, the waveforms of the sAIC and the longAIC have enough margins to show the whole signal. The integrated charge from the longAIC was 0.31 µC/Cycle which corresponds to the 450 W lost at the collimators.

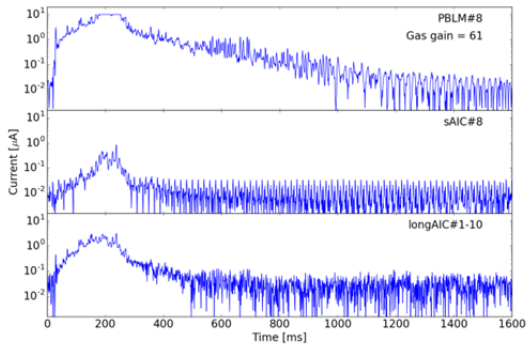

Figure 5: Waveforms of the PBLM, the sAIC, and the longAIC installed at the Injector and Collimator section.

The dual detector system of the PBLM and the sAIC can compensate for the weakness of the PBLM and shows wide dynamic range. At each bias setting the dynamic range is about 80 dB for integrated charge data, and an appropriate bias setting can expands the total dynamic range. The upper limit of the integrated charge of the sAIC can be estimated greater than 0.1 µC/Cycle considering the present margin. Including the data of residual dose measurements, the net dynamic range is now wider than 160 dB.

SUMMARY

The new BLM system for the J-PARC MR has been operating successfully since last summer. Thanks to the high gas gain performance of the PBLM and the combined use of the sAIC, the system dynamic range is now wider than 160 dB. The present signal rise time of 17 µs is slower than the initial design goal of 10 µs. However it is likely to be fast enough to ensure that the MPS system will dump the beam within 100 µs. The output signal of the longAIC was calibrated using the controlled beam losses at the Collimators and Arc A and Arc B. The beam power loss in the Injector and Collimator section was 450 W in the FX mode operation which outputs 460 kW beam power.

To improve signal-to-noise ratio of the waveform data obtained, further studies are needed. We are now designing another detector system for a new BLM that will operate with bandwidth of more than 200 kHz.

REFERENCES

[1] K. Satou *et al.*, Proc. of IPAC2012 (2012), p. 837.

[2] H. Nakagawa *et al.*, Proc. of ICALEPCS2009 (2009) p406.

[3] Accelerator Technical Design Report for J-PARC, KEK Report 2002-13, Mar. 2003.

[4] M. J. Shirakata *et al.*, Proc. of HB2016 (2016) p. 543.

[5] T. Toyama *et al.*, Proc. of HB2008 (2008) p. 450.

[6] Y. H. Chin *et al.*, Proc. of PAC2013 (2013) p. 23.

[7] S. Lee *et al.*, Proc. of EPAC2004 (2004) p. 2667.

[8] K. Satou *et al.*, Proc. of HB2008 (2008) p. 472.

[9] H. Sipila, V. Vanha-honko, Nucl. Instr. And Meth. 153 (1978) 461.

[10] K. Satou *et al.*, Proc. of IPAC2014 (2014) p. 3547.

ISBN 978-3-95450-182-3